Journal of Catalysis 260 (2008) 157–163

Contents lists available at ScienceDirect

Journal of Catalysis

www.elsevier.com/locate/jcat

Application of the unique redox properties of magnesium *ortho*-vanadate incorporated with palladium in the unsteady-state operation of the oxidative dehydrogenation of propane

S. Sugiyama [a,b,c,*], Y. Hirata [b], K. Nakagawa [a,b,c], K.-I. Sotowa [a,b,c], K. Maehara [d], Y. Himeno [d], W. Ninomiya [e]

[a] Department of Advanced Materials, Institute of Technology and Science, The University of Tokushima, Minamijosanjima, Tokushima 770-8506, Japan
[b] Department of Geosphere Environment and Energy, Center for Frontier Research of Engineering, The University of Tokushima, Minamijosanjima, Tokushima 770-8506, Japan
[c] Department of Chemical Science and Technology, The University of Tokushima, Minamijosanjima, Tokushima 770-8506, Japan
[d] Corporate Research Laboratories, Mitsubishi Rayon Co. Ltd., 20-1 Miyuki-cho, Otake, Hiroshima 739-0693, Japan
[e] Research and Development Administration Department, Mitsubishi Rayon Co. Ltd., 6-41, Konan 1-chome, Minato-ku, Tokyo 108-8506, Japan

ARTICLE INFO

Article history:
Received 30 July 2008
Revised 22 September 2008
Accepted 22 September 2008
Available online 15 October 2008

Keywords:
Oxidative dehydrogenation
Propane
Magnesium vanadates
Palladium
Redox
EXAFS
^{51}V MAS NMR
Unsteady-state operation

ABSTRACT

The oxidative dehydrogenation of propane on Pd^{2+}-incorporated magnesium *ortho*-vanadate (Pd-*ortho*-MgVO) was examined, despite the long-held belief that magnesium *ortho*-vanadate ($Mg_3V_2O_8$) demonstrates scant catalytic activity in oxidative dehydrogenation. At 0.75 h on-stream, a higher activity than that on magnesium *pyro*-vanadate (monoclinic $Mg_2V_2O_7$), which is believed to be one of the more active catalysts for oxidative dehydrogenation, was observed using 5% Pd-*ortho*-MgVO. Unfortunately, the higher catalytic activity decreased with time on stream due to the rapid abstraction of lattice oxygen from 5% Pd-*ortho*-MgVO. Although the abstracted lattice oxygen was not regenerated during oxidative dehydrogenation in the presence of excess gaseous oxygen, it was easily regenerated during reoxidation in the absence of propane in the feedstream. Redox cycles of palladium and vanadium species during the catalytic reaction and reoxidation were confirmed using extended X-ray absorption fine structure around the Pd K-edge and ^{51}V magic-angle spinning nuclear magnetic resonance, respectively. The results of the present study suggest that the higher catalytic activity observed using 5% Pd-*ortho*-MgVO at 0.75 h on-stream can be maintained by using an unsteady-state operation in combination with the catalytic reaction and catalyst reoxidation.

1. Introduction

Because some reviews suggest that catalysts containing vanadium species are effective active catalysts for the oxidative dehydrogenation of propane [1–3], various types of vanadium-containing catalysts are still used for the reaction [4–6]. Among vanadium-containing catalysts, magnesium *meta*-, *pyro*-, and *ortho*-vanadates (MgV_2O_6, monoclinic $Mg_2V_2O_7$, and $Mg_3V_2O_8$) are active catalysts for the oxidative dehydrogenation of propane. Magnesium *pyro*-vanadates have the highest activity; *ortho*-vanadates, the lowest activity [1,7]. The ease of removal of the lattice oxygen contained in V=O and/or V–O–V of those magnesium vanadates explains their high catalytic activity in the oxidative dehydrogenation of propane [1,8,9]; however, it should be noted that the structural stability of *pyro*-magnesium vanadate, particularly during the redox cycle, evidently is lower than that of magnesium ortho-vanadate [10]. For example, both monoclinic $Mg_2V_2O_7$ and $Mg_3V_2O_8$ were converted to a mixture of MgO and Mg_2VO_4 during the oxidative dehydrogenation of propane without gaseous oxygen in the feed, indicating that vanadium was reduced from V^{5+} to V^{4+}. When the mixture obtained from monoclinic $Mg_2V_2O_7$ was reoxidized with gaseous oxygen, triclinic $Mg_2V_2O_7$ formed, although not in its original monoclinic phase. The activity of the newly formed $Mg_2V_2O_7$ for the oxidative dehydrogenation of propane was significantly less than that of fresh monoclinic $Mg_2V_2O_7$. In contrast, $Mg_3V_2O_8$ was completely regenerated from the reoxidation of the mixture obtained from $Mg_3V_2O_8$. As a result, the activity for the oxidative dehydrogenation of propane was maintained at a level comparable to that of fresh $Mg_3V_2O_8$. Thus, from a practical standpoint, catalytic activity can be improved by using structurally stable $Mg_3V_2O_8$, rather than structurally unstable monoclinic $Mg_2V_2O_7$.

To control the removal of the lattice oxygen in magnesium vanadates, Ca^{2+}, Cu^{2+}, and Fe^{3+} were incorporated into the magnesium vanadates [11–13]. Catalytic activity certainly is related to the ease of abstraction of the lattice oxygen from the incorporated catalysts; however, the characteristic advantages of the incorpo-

* Corresponding author at: Department of Advanced Materials, Institute of Technology and Science, The University of Tokushima, Minamijosanjima, Tokushima 770-8506, Japan. Fax: +81 88 656 7432.
E-mail address: sugiyama@chem.tokushima-u.ac.jp (S. Sugiyama).

0021-9517/$ – see front matter
doi:10.1016/j.jcat.2008.09.015

rated cations on catalytic activity, such as enhanced propylene yield, were not observed. This result indicates that a cation that can increase the numbers of mobile lattice oxygen atoms should be examined.

The purpose of the present study was to examine the effect of introducing Pd^{2+} into magnesium ortho-vanadate on the catalytic activity for the oxidative dehydrogenation of propane. Because the Pd^{2+}-incorporated catalysts showed remarkable redox cycle activity in a shorter time-on-stream, our investigation focused on the mobility of lattice oxygen and the redox nature of the palladium and vanadium species using quadrupole mass spectrometry (Q-mass), extended X-ray absorption fine structure (EXAFS) analysis at the Pd K-edge, and ^{51}V solid-state magic-angle spinning nuclear magnetic resonance (^{51}V MAS NMR). Furthermore, to maintain this significantly enhanced activity during a shorter time on stream, an unsteady-state operation combined with the catalytic reaction and reoxidation of the catalyst was investigated using the Pd^{2+}-incorporated catalyst.

2. Experimental

2.1. Catalyst preparation

Magnesium *ortho*-vanadate with Pd^{2+} incorporated (*x*% Pd-*ortho*-MgVO; x = 100Pd/(Pd + Mg) (atomic ratio)) was prepared from $Mg(OH)_2$ (Wako Pure Chemical Industries, Ltd., Osaka, Japan), an aqueous $Pd(NO_3)_2$ solution (24.41% by weight, N.E. Chemcat Corporation, Tokyo, Japan), and NH_4VO_3 (Kanto Chemical Co. Inc., Tokyo, Japan). The preparation procedure was essentially identical to that reported by Sam et al. for the parent magnesium *ortho*-vanadate [7]. An aqueous mixture of a fine powder of $Mg(OH)_2$ and $Pd(NO_3)_2$ was added to an 1% ammonia solution of NH_4VO_3; the reagent amounts were adjusted to the atomic ratios of the corresponding catalysts. The suspension was evaporated under stirring and then dried at 353 K. The resulting solid was ground into a fine powder, calcined at 823 K for 6 h, and then recalcined at 973 K for 10 h. Each solid was finely ground between calcinations. Magnesium *pyro*-vanadate incorporated with Pd^{2+} (5% Pd-*pyro*-$Mg_2V_2O_7$) also was prepared following a procedure similar to that used for the corresponding Pd-*ortho*-MgVO. In the present study, PdO, a mixed catalyst (5% PdO + 95% $Mg_3V_2O_8$), and a supported catalyst (5% Pd/$Mg_3V_2O_8$) also were used. After calcination at 973 K for 3 h, PdO (Wako) was used to test catalytic activity. The mixed catalyst was prepared by mechanical mixing of the calcined PdO and $Mg_3V_2O_8$ prepared in the present study. The supported catalyst was prepared from $Mg_3V_2O_8$ by impregnation of an aqueous $Pd(NO_3)_2$ solution, followed by calcination at 973 K for 3 h.

2.2. Catalytic activity test

The catalyst thus obtained (particles of 0.85–1.70 mm) was used in a fixed-bed continuous-flow reactor operated at atmospheric pressure. Unless stated otherwise, the catalyst was heated to the reaction temperature (723 K) under a continuous flow of helium, then held at this temperature under a 25 mL/min flow of oxygen for 1 h. Typical reaction conditions were $W = 0.5$ g, $P(C_3H_8) = 14.4$ kPa, $P(O_2) = 4.1$ kPa, and $F = 30$ mL/min; equilibration to atmospheric pressure was provided by helium. No homogeneous oxidation of propane was observed under the study conditions. The reaction was monitored by a online gas chromatograph with a thermal conductivity detector (GC-8APT, Shimadzu, Kyoto, Japan). The conversion of propane was calculated from the products and the propane introduced into the feedstream. The selectivity was calculated from the conversion of propane to each product on a carbon basis. The carbon mass balance was 100 ± 5%. The reaction rate per unit of surface area was estimated as the rate ($r = FC_0X_A/W$, where F, C_0, X_A, and W were the flow rate, initial concentration of C_3H_8, conversion of C_3H_8 and catalyst weight, respectively) per catalyst surface area [14]. For continuous analysis of the reaction, an effluent gas from the reactor was introduced into the Q-mass (Pfeiffer OmniStar-s, Hakuto Co., Tokyo, Japan).

2.3. Characterization

The catalysts were characterized using X-ray diffraction (XRD; RINT 2500X using monochromatized Cu$K\alpha$ radiation, Rigaku Co., Tokyo, Japan). X-ray photoelectron spectroscopy (XPS; ESCA-1000AX, Shimadzu) was performed using Mg$K\alpha$ radiation. ^{51}V MAS NMR spectra were obtained using an Avance DSX300 (Bruker BioSpin K. K., Osaka, Japan) with an external reference of 0.16 M $NaVO_3$ (Wako) solution at −574 ppm at room temperature and a spinning rate of 25 kHz. Specific surface areas were calculated from adsorption isotherms obtained with a conventional BET nitrogen adsorption apparatus (BELSORP-18SP, Bell Japan, Inc., Osaka, Japan). Analysis of EXAFS near the Pd K-edge was carried out at the High-Energy Research Organization with a storage ring current of approximately 400 mA (6.5 GeV). The X-ray was monochromatized with Si(311) at an NW-10A station. The absorption spectra were observed using ionization chambers in transmission mode. Samples containing palladium species were diluted with BN (Wako) and compressed to a diameter of 13 mm. The photon energy was scanned in the range of 24,080–25,600 eV for a Pd K-edge. The EXAFS data were analyzed using the EXAFS analysis program REX (Rigaku). Fourier transformation of k^3-weighted EXAFS oscillation was performed in the range of 0.4–1.6 nm^{-1}. Inverse Fourier-transformed data for Fourier peaks were analyzed using a curve-fitting method, with phase shift and amplitude functions derived from FEFF 8.0 [15].

3. Results and discussion

3.1. Catalytic activities on Pd-ortho-MgVO

Four types of Pd-*ortho*-MgVO were prepared. The XRD pattern of the undoped catalyst was essentially identical to the reference pattern of $Mg_3V_2O_8$ (JCPDS 37-0351) (Fig. 1A), whereas those of the three Pd-*ortho*-MgVO were matched to the mixture of $Mg_3V_2O_8$ and PdO (JCPDS 41-1107) (Figs. 1B–1D). It should be noted that the intensity of the PdO signal increased with increasing Pd content.

Fig. 2 shows the time course of the propylene yields for various Pd-*ortho*-MgVO. Table 1 gives the conversion, selectivity, reaction rate per unit of surface area, and surface area. Although the C_3H_6 yield decreased significantly with time-on-stream, the yield increased with Pd loading, particularly at the initial time-on-stream. At 0.75 h on-stream, the propylene yields were 5% Pd-*ortho*-MgVO (7.8%) > *pyro*-$Mg_2V_2O_7$ (7.1%) [12] > *ortho*-$Mg_3V_2O_8$ (2.9%). These results show that incorporation of the Pd^{2+} species into $Mg_3V_2O_8$ resulted in enhanced activity for the oxidative dehydrogenation of propane under equivalent reaction conditions. However, as shown in Fig. 1, PdO and $Mg_3V_2O_8$ were detected in Pd-*ortho*-MgVO using XRD. Therefore, either PdO itself or the synergistic effects of the combination of PdO and $Mg_3V_2O_8$, in bulk or on the surface, may contribute to the enhanced initial activity on Pd-*ortho*-MgVO. Furthermore, vanadate may be present on the surface of $Mg_3V_2O_8$ as a supported catalyst. Consequently, the activities on PdO and on the binary oxides, 5% PdO and 95% $Mg_3V_2O_8$ (by weight), together with that on the supported catalyst (5% Pd/$Mg_3V_2O_8$), were examined (Fig. 3 and Table 1). As shown in Fig. 3, relatively stable and low activity was observed on both PdO and binary oxides. In particular, the yield of C_3H_6 on PdO was about 25% of that on 5% Pd-*ortho*-MgVO, while that on the binary oxide was almost the

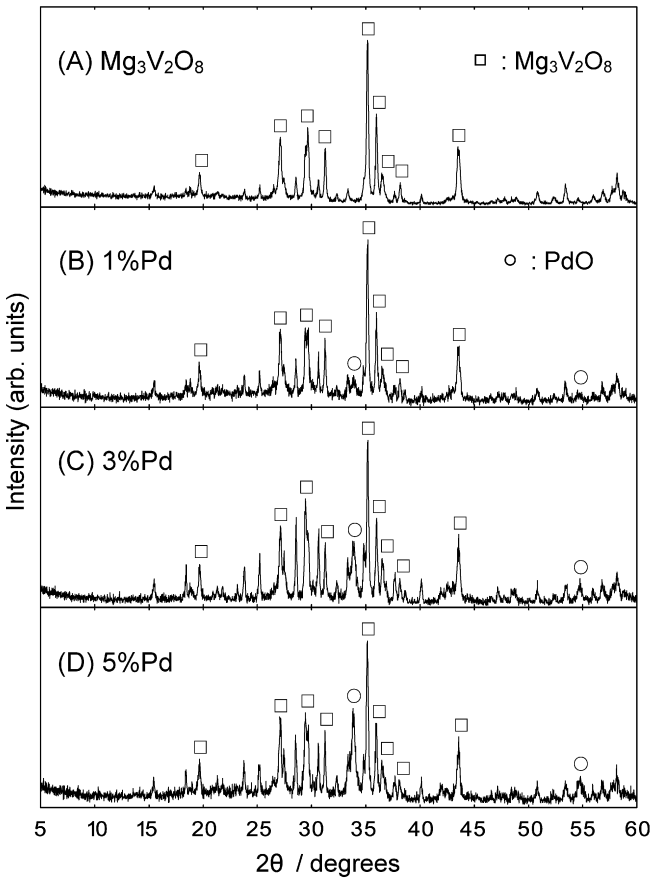

Fig. 1. XRD patterns of various Pd-*ortho*-MgVO catalysts before use for the oxidative dehydrogenation of propane.

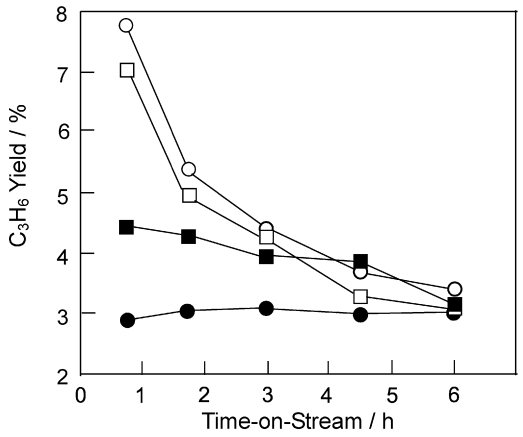

Fig. 2. C_3H_6 yield on $Mg_3V_2O_8$ and various Pd-*ortho*-MgVO catalysts. Symbols: (●) $Mg_3V_2O_8$; (■) 1% Pd-*ortho*-MgVO; (□) 3% Pd-*ortho*-MgVO; (○) 5% Pd-*ortho*-MgVO.

same as that on $Mg_3V_2O_8$. This result indicates that the location of Pd^{2+} in Pd-*ortho*-MgVO is different from that in the binary oxide. Of interest, the C_3H_6 yields on 5% Pd/$Mg_3V_2O_8$ decreased with time-on-stream, similar to results observed for 5% Pd-*ortho*-MgVO (Fig. 3 and Table 1). Although 5% Pd/$Mg_3V_2O_8$ showed higher C_3H_8 conversion and lower C_3H_6 selectivity compared with 5% Pd-*ortho*-MgVO, the location of vanadium species on the supported catalyst was similar to that of the vanadium species in 5% Pd-*ortho*-MgVO. It should be noted that the effect of Pd^{2+} in Pd-*ortho*-MgVO on the catalytic activity was not observed on 5% Pd-*pyro*-$Mg_2V_2O_7$. The C_3H_6 yields on Pd-*pyro*-$Mg_2V_2O_7$ were 4.2 at 0.75 h and 2.7%

Table 1
Surface areas and catalytic activities on $Mg_3V_2O_8$, Pd-*ortho*-MgVO catalysts, PdO, the mixed catalyst (5% PdO + 95% $Mg_3V_2O_8$) and the supported catalyst (5% Pd/$Mg_3V_2O_8$) at 0.75 and 6 h on-stream.

Pd (%) or catal.	S.A.[a] (m^2/g)	Conversion (%)		Selectivity (%)			Rate[b]
		C_3H_8	O_2	C_3H_6	CO_2	CO	
0%	7.9	5.0	46.0	58.1	24.0	17.9	2.27×10^{-6}
		(4.8)	(41.0)	(62.4)	(21.4)	(16.2)	(2.18×10^{-6})
1%	8.3	9.1	90.0	49.1	40.0	10.9	3.93×10^{-6}
		(7.3)	(90.0)	(42.7)	(49.1)	(8.2)	(3.15×10^{-6})
3%	9.5	12.2	92.0	57.7	32.0	10.3	4.60×10^{-6}
		(7.9)	(92.0)	(38.6)	(53.5)	(7.9)	(2.98×10^{-6})
5%	7.8	13.4	92.0	57.9	29.7	12.4	6.15×10^{-6}
		(8.9)	(92.0)	(38.0)	(52.5)	(9.5)	(4.09×10^{-6})
PdO	1.2	6.5	92.0	26.7	62.4	11.0	19.40×10^{-6}
		(6.2)	(92.0)	(25.9)	(62.5)	(11.5)	(18.51×10^{-6})
Mixed	9.7	7.2	92.0	35.8	50.6	13.6	2.66×10^{-6}
		(7.8)	(93.0)	(39.5)	(53.2)	(7.2)	(2.88×10^{-6})
Supported	8.2	25.0	100.0	32.9	39.7	27.5	10.92×10^{-6}
		(10.9)	(100.0)	(23.6)	(70.9)	(5.6)	(4.76×10^{-6})

[a] Surface area (m^2/g).
[b] Values in parentheses: activities at 6 h on-stream.

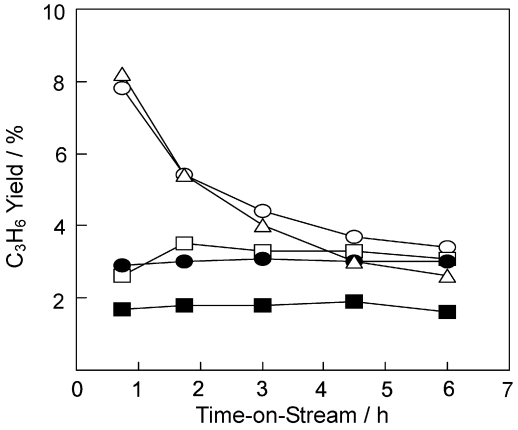

Fig. 3. C_3H_6 yield on $Mg_3V_2O_8$ and related catalysts. Symbols: (●) $Mg_3V_2O_8$; (■) PdO; (□) 5% PdO + 95% $Mg_3V_2O_8$; (○) 5% Pd-*ortho*-MgVO; (△) 5% Pd/$Mg_3V_2O_8$.

at 6 h on-stream, noticeably smaller than that on *pyro*-$Mg_2V_2O_7$ (7.1%) [12]. To examine the role of Pd^{2+} in Pd-*ortho*-MgVO, the remainder of this study focused on 5% Pd-*ortho*-MgVO.

3.2. Abstraction and incorporation of lattice oxygen in 5% Pd-ortho-MgVO

As described above, introducing Pd^{2+} into $Mg_3V_2O_8$ significantly enhanced the catalytic activity for the oxidative dehydrogenation of propane at initial time-on-stream. This result indicates that the redox nature of the catalyst is controlled by the introduction of Pd^{2+}, as we reported in our previous paper on the effect of the introduction of various divalent cations into magnesium vanadates during the oxidation of propane [11–13]. Indeed, XRD patterns of 5% Pd-*ortho*-MgVO before and after oxidative dehydrogenation (Fig. 2) show that $Mg_3V_2O_8$ and PdO detected in the fresh catalyst were reduced to Mg_2VO_4 and metallic Pd after the reaction (see below). Consequently, to determine the abstraction rate of lattice oxygen from $Mg_3V_2O_8$ and 5% Pd-*ortho*-MgVO to form the vacancy and the incorporation rate of gaseous oxygen into the vacancy, we carried out reduction and reoxidation experiments using these two catalysts. Our previous studies used a feedstream consisting of C_3H_8 as the reduction gas [11–13,22]; here, however, the feedstream consisted of H_2, to avoid both carbon deposition during the reduction experiment and oxidation of carbon deposition during the reoxidation experiment, which are unfavorable for the

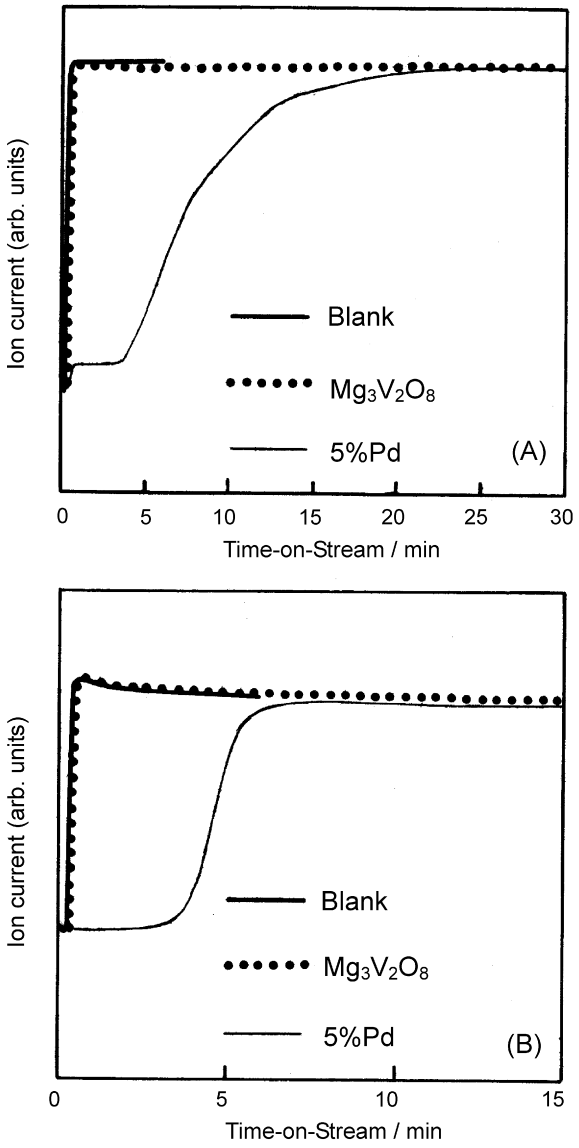

Fig. 4. Hydrogen and oxygen responses ((A) and (B), respectively) in effluent gas from $Mg_3V_2O_8$ and 5% Pd-*ortho*-MgVO.

quantitative analysis of the abstraction rates of lattice oxygen from $Mg_3V_2O_8$ and 5% Pd-*ortho*-MgVO to form the vacancy and the incorporation rate of gaseous oxygen into the vacancy. First, a reduction gas consisting of H_2 (14.4 kPa) diluted with He was introduced at a flow rate of $F = 30$ ml/min into $Mg_3V_2O_8$ and 5% Pd-*ortho*-MgVO (each 0.5 g) at 723 K. A quadrupole mass spectrometer was used to analyze the hydrogen response in the effluent gas from these catalysts (Fig. 4A). The hydrogen response using $Mg_3V_2O_8$ was essentially identical to the blank test, in which hydrogen was detected just after introduction of the hydrogen gas into $Mg_3V_2O_8$ (Fig. 4A). In the blank test, the reactor was filled with quartz wool instead of the catalyst; thus, reduction of $Mg_3V_2O_8$ with hydrogen gas was difficult. But hydrogen was detected after 3 min using 5% Pd-*ortho*-MgVO, and the amount of hydrogen in the effluent gas increased gradually with time-on-stream. This result indicates that lattice oxygen in 5% Pd-*ortho*-MgVO was readily abstracted to react with hydrogen. Based on the curve described in Fig. 4A, 14.4% of the lattice oxygen in 5% Pd-*ortho*-MgVO was abstracted during the 30-min reduction. After the reduction, the reduced catalysts, $Mg_3V_2O_8$ and 5% Pd-*ortho*-MgVO, were reoxidized at 723 K with a reoxidation gas consisting of O_2 (14.4 kPa) diluted with He at a flow rate of $F = 30$ ml/min. Quadrupole mass spectrometry was used to determine the oxygen response in the effluent gas from these catalysts (Fig. 4B). Again, the oxygen response using $Mg_3V_2O_8$ that had been previously treated with H_2 gas was essentially identical to that of the blank test, in which oxygen was detected just after oxygen gas was introduced into $Mg_3V_2O_8$ (Fig. 4B). Therefore, the reduction followed by reoxidation of $Mg_3V_2O_8$ was difficult to achieve, and it resulted in low activity for the oxidative dehydrogenation. In contrast, oxygen was detected after 3 min using 5% Pd-*ortho*-MgVO that had been previously treated with H_2 gas. The amount of oxygen in the effluent gas increased gradually with increasing time-on-stream (Fig. 4B). This result indicates that oxygen was readily introduced into the vacancy formed in 5% Pd-*ortho*-MgVO during the reduction. Based on the curve shown in Fig. 4B, 14.9% of the oxygen, corresponding to the amount of abstracted oxygen (14.4%), was introduced into the reduced 5% Pd-*ortho*-MgVO during reoxidation for 15 min. Therefore, the facile redox nature of 5% Pd-*ortho*-MgVO was confirmed. In particular, the facile abstraction of lattice oxygen from the catalyst may contribute to the unique catalytic properties, such as the remarkable increase in the initial activity and the decrease in the activity with time-on-stream (Figs. 2 and 3).

3.3. Redox nature of vanadium and palladium species in 5% Pd-ortho-MgVO

Because redox (i.e., abstraction and incorporation of lattice oxygen) was readily achieved using 5% Pd-*ortho*-MgVO, as described above, we also examined the compensation for the cation valence (vanadium and palladium species) in the catalyst occurring simultaneously with the redox. As shown in Fig. 5, $Mg_3V_2O_8$ and PdO that were detected in 5% Pd-*ortho*-MgVO before the reaction (Fig. 5A) were converted into Mg_2VO_4 (JCPDS 50-0532), metallic Pd (JCPDS 46-1043), and MgO (JCPDS 45-0946) (Fig. 5B). This result indicates that the vanadium and palladium species were reduced from 5+ and 2+ to 4+ and 0, respectively, during the oxidative dehydrogenation of propane under typical reaction conditions. It should be noted that the activity of the reduced 5% Pd-*ortho*-MgVO was relatively low after 6 h on-stream, as shown in Fig. 2. When 5% Pd-*ortho*-MgVO, described in Fig. 5B, was reoxidized with O_2 (25 ml/min) at 723 K for 1 h, the regeneration of $Mg_3V_2O_8$ and PdO (i.e., the regeneration of V^{5+} and Pd^{2+}) was confirmed, while MgO was still present (Fig. 5C). The surface analyses of the samples used in Fig. 5A, B and C by XPS (Fig. 6) also revealed that the Pd-species was converted from Pd^{2+} (binding energy due to Pd $3d_{5/2}$: 337.3 eV) [16–18] (Table 2A) to Pd^0 (335.6 eV) [19] (Table 2B), followed by the regeneration of Pd^{2+} (337.4 eV) (Table 2C), as observed on XRD (Fig. 5). The XPS due to V $2p_{3/2}$ was detected at nearly identical binding energies between 517.6 and 517.9 eV, regardless of the reaction conditions (Table 2). As we reported previously [13], binding energies of 517.85, 517.5, and 516.8 eV were reported for V^{5+} [19], whereas a chemical shift of approximately 1 eV was detected between V^{5+} (V_2O_5) and V^{4+} (VO_2) in XPS (516.8 and 515.7 eV, respectively) [19]. Therefore, although V^{4+} was detected as Mg_2VO_4 by XRD (Fig. 5), the valency of vanadium on the catalyst surface was approximately 5+ regardless of the conditions, due to the supply of the oxygen species from the bulk or gas phase to the catalyst surface.

As shown in Figs. 1 and 5, various identified and unidentified XRD peaks were detected. The possibility of formation of small amounts of various magnesium vanadates (e.g., MgV_2O_6, triclinic $Mg_2V_2O_7$, monoclinic $Mg_2V_2O_7$) cannot be excluded [7], although peaks characteristic of these compounds were not identified in the present study due to ambiguity. It should be noted that the XRD pattern shown in Fig. 5B is similar to that of a mixture of MgO and $Mg_3V_2O_6$ [20]. $Mg_3V_2O_6$, in which V^{3+}, but not V^{4+}, is present,

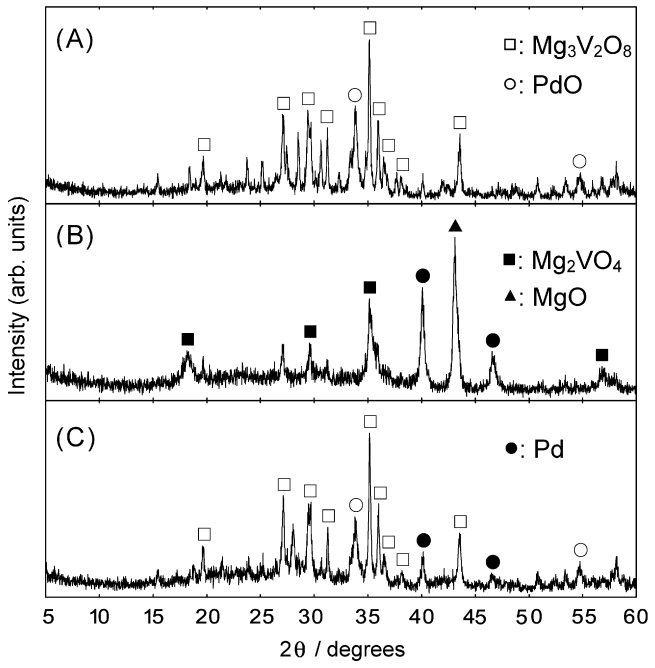

Fig. 5. XRD patterns of 5% Pd-*ortho*-MgVO used in various conditions. (A) Before the reaction. (B) After the reaction under typical reaction conditions. (C) After re-oxidation with gaseous O_2 (25 ml/min) for 1 h at 723 K.

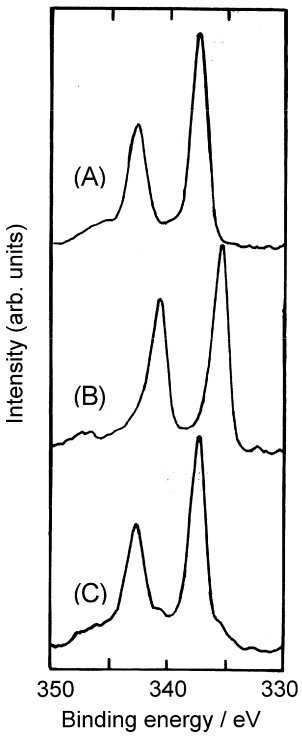

Fig. 6. XPS of Pd 3d of 5% Pd-*ortho*-MgVO used in various conditions. (A) Before the reaction. (B) After the reaction under typical reaction conditions. (C) After re-oxidation with gaseous O_2 (25 ml/min) for 1 h at 723 K.

Table 2
Binding energies detected by XPS for $Mg_3V_2O_8$ and 5% Pd-*ortho*-MgVO used for various conditions.

Conditions	Binding energy (eV)			
	Mg 2s	Pd $3d_{5/2}$	V $2p_{3/2}$	O 1s
(A)	88.5	337.3	517.7	530.4
(B)	88.7	335.6	517.9	530.8
(C)	88.7	337.4	517.6	530.7

(A) Before the reaction. (B) After the reaction under the typical reaction conditions. (C) After re-oxidation with gaseous O_2 (25 ml/min) for 1 h at 723 K.

has been obtained from the careful reduction of $Mg_3V_2O_8$ [20,21]. Moreover, poor crystallinity of magnesium vanadate was detected (Fig. 5B), indicating that information on amorphous species may not be reflected in the XRD. For example, reduction using hydrocarbons (C_mH_n) has been suggested, as follows:

$$Mg_3V_2O_8 + C_mH_n \rightarrow 3Mg_2VO_4 + VO_2 + mCO_x + 0.5nH_2O. \quad (1)$$

Although Mg_2VO_4 was detected using XRD, information on VO_2 was not obtained from XRD or XPS. Therefore, in the present system, it is important to detect a change in the valency of the redox species and to obtain information on amorphous species using other characterization procedures.

To confirm the redox properties of vanadium and palladium species during the cycle used to obtain the results shown in Figs. 5A, 5B and 5C, 5% Pd-*ortho*-MgVO was analyzed using ^{51}V MAS NMR and Pd K-edge EXAFS. ^{51}V MAS NMR is suitable for analyzing the redox nature of vanadium species, because diamagnetic V^{5+} affords evident NMR signals, whereas reduced vanadium species (V^{4+} and/or V^{3+}) affords broad and weak signals [13,22]. Fig. 7 shows the ^{51}V MAS NMR of 5% Pd-*ortho*-MgVO, which can be described as follows: (A) before the reaction, (B) after the reaction under the typical reaction conditions, and (C) after the reoxidation of the sample (B) at 723 K for 1 h with gaseous O_2 (25 ml/min). It should be noted that these NMR results are described using a noise level similar to the baseline level. An evident NMR signal due to V^{5+} was detected at −552 ppm from the catalyst before the reaction (Fig. 7A); however, the intensity of the signal decreased after the reaction under typical reaction conditions, indicating that the vanadium species was reduced even with gaseous oxygen in the feedstream (Fig. 7B). As we reported previously [22], the reduction of a vanadium species (V^{5+}) in undoped *ortho*-MgVO ($Mg_3V_2O_8$) was very difficult, because V^{5+} was still detected even after the reaction of $Mg_3V_2O_8$ using the feedstream in the absence of gaseous oxygen. Therefore, the introduction of Pd^{2+} into $Mg_3V_2O_8$ enhanced the reductive nature of the vanadium species.

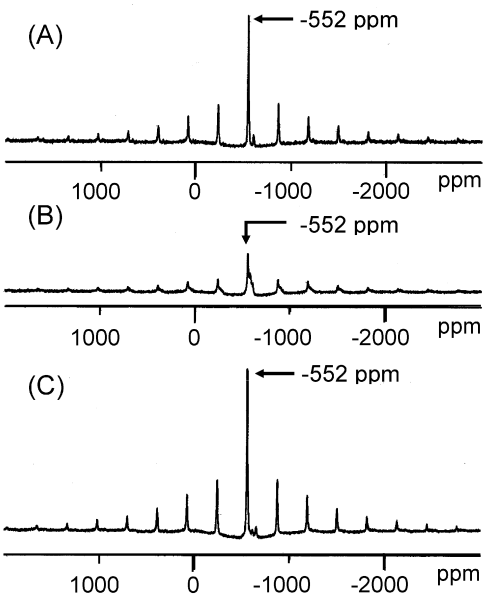

Fig. 7. ^{51}V MAS NMR of 5% Pd-*ortho*-MgVO used in various conditions. (A) Before the reaction. (B) After the reaction under typical reaction conditions. (C) After re-oxidation with gaseous O_2 (25 ml/min) for 1 h at 723 K.

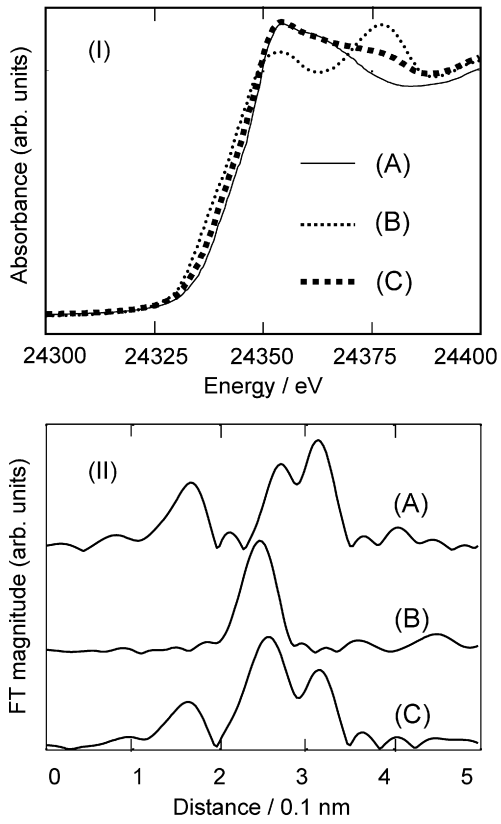

Fig. 8. Pd K-edge XANES spectra (I) and the corresponding Fourier transformation (II) of EXAFS of 5% Pd-*ortho*-MgVO used in various conditions. (A) Before the reaction. (B) After the reaction under typical reaction conditions. (C) After re-oxidation with gaseous O_2 (25 ml/min) for 1 h at 723 K.

As shown in Fig. 7C, after reoxidation of the sample (B), the intensity of the present NMR signal was completely regenerated by the intensity level of the sample (A), or, rather, it became greater than that shown in Fig. 7A. This result indicates that the reduced vanadium species was readily oxidized. Therefore, the redox nature of vanadium species was noticeably improved by the incorporation of Pd^{2+} into $Mg_3V_2O_8$. Fig. 8 shows the Pd K-edge XANES spectra of the samples (A), (B), and (C) and the corresponding Fourier transformation around the Pd K-edge. The order of the absorption edge was as follows: sample A > sample C > sample B (Fig. 8(I)). This result indicates that the oxidized Pd species in sample A was reduced during the reaction to form the reduced Pd species (sample B), which was partially oxidized after reoxidation (sample C). The corresponding Fourier transformation around the Pd K-edge provides additional information about the redox nature of the palladium species (Fig. 8(II)). In sample A, three signals similar to those from PdO were detected in our study (not shown) and in another study [23], indicating that the Pd species in sample A was Pd^{2+}. After the reaction, the three peaks appeared as one signal, as shown by sample B, which was essentially identical to that of metallic Pd [23,24]; therefore, the Pd species was completely reduced to metallic Pd during the reaction. But the metallic Pd species was not completely oxidized to Pd^{2+} after the reoxidation of sample B, because the Fourier transformation of sample C showed both Pd^{2+} and metallic Pd peaks (Fig. 8(II)). Therefore, the Pd species in 5% Pd-*ortho*-MgVO could be readily reduced during the reaction, even with gaseous O_2 in the feedstream. In contrast, the reduced Pd species in the catalyst was barely reoxidized under the conditions that resulted in complete reoxidation of the corresponding vanadium species (Fig. 7C).

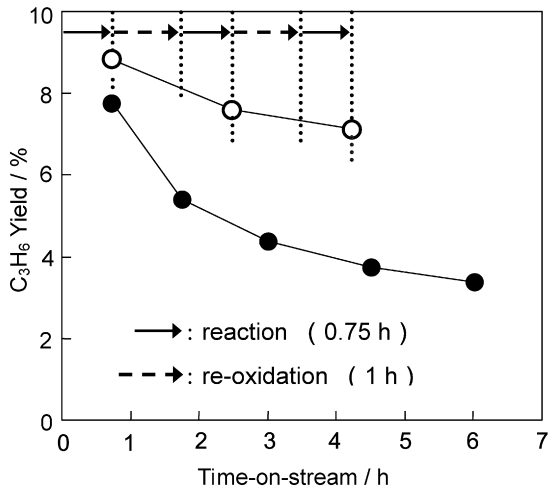

Fig. 9. Comparison of the yields of C_3H_6 under steady-state and unsteady-state conditions.

3.4. Unsteady-state operation on 5% Pd-ortho-MgVO

As described above, the vanadium and palladium species in Pd-*ortho*-MgVO could be readily reduced in the reaction, even with gaseous oxygen in the feedstream, followed by complete reoxidation and partial reoxidation, respectively. Therefore, the ready reduction of the catalyst decreased the activity with time-on-stream, as shown in Fig. 2. The combination of the reaction and reoxidation during the oxidative dehydrogenation of propane, an unsteady-state operation, may improve the activity with time-on-stream. Thus, continuous operation of the oxidative dehydrogenation of propane under typical reaction conditions, followed by the reoxidation with gaseous O_2 (25 ml/min) for 1 h at 723 K was recycled twice (unsteady-state operation). Comparing the results of this procedure with those of normal oxidative dehydrogenation under typical reaction conditions (i.e., steady-state conditions), clearly shows that under the unsteady-state conditions, the catalytic activity was greater, whereas the rate of the decrease was suppressed (Fig. 9). Unfortunately, the decreased activity under unsteady-state conditions was not completely reversed, due to the poor reoxidation nature of metallic Pd species that formed during the reaction with gaseous oxygen in the feedstream. An advanced technique that allows interchange of the reactant stream and reoxidation stream and heating only on the catalyst surface is needed to overcome these disadvantages. This cannot be achieved using a typical fixed-bed continuous-flow reactor. Consequently, we are now in the process of developing a “microreactor” for the present system [25]. Our findings show that the use of unsteady-state operations in the oxidative dehydrogenation of alkanes is another possible procedure for the efficient production of partial oxidation products.

4. Conclusion

The initial activity for the oxidative dehydrogenation of propane was enhanced by the introduction of Pd^{2+} into magnesium vanadate, whereas the activity was evidently decreased with time-on-stream due to the easily reducible nature of the vanadium and palladium species. The decrease in activity was partially reversed by use of unsteady-state operation; the reduced Pd species that formed during the reaction were barely reoxidized by treatment with oxygen. The use of the unsteady-state operation may be another possible procedure for the oxidative dehydrogenation of alkanes.

Acknowledgments

This work was funded by Grants-in-Aid for Scientific Research (A) KAKENHI 20241020 (to S.S.) and (B) KAKENHI 19360360 (to K.S.). The XAFS study was performed with the approval of the Photon Factory Advisory Committee of the High-Energy Research Organization (Proposal 2007G007).

References

[1] H.H. Kung, Adv. Catal. 40 (1994) 1.
[2] E.A. Mamedov, V.C. Corberan, Appl. Catal. A 127 (1995) 1.
[3] F. Cavani, F. Trifiro, Catal. Today 24 (1995) 307.
[4] I. Rossetti, L. Fabbrini, N. Ballarini, C. Olova, F. Cavani, A. Cericola, B. Bonelli, M. Piumetti, E. Garrone, H. Dyrbeck, E.A. Blekkan, L. Forni, J. Catal. 256 (2008) 45.
[5] X. Rozanska, E.V. Kondratenko, J. Sauer, J. Catal. 256 (2008) 84.
[6] B. Mitra, I.E. Wache, G. Deo, J. Catal. 240 (2006) 151.
[7] D.S.H. Sam, V. Soenen, V.C. Volta, J. Catal. 123 (1990) 435.
[8] M.A. Pepera, J.L. Callahan, M.J. Desmond, E.C. Milberger, P.R. Blum, N.J. Bremer, J. Am. Chem. Soc. 107 (1985) 4883.
[9] Y. Yoshimura, Catal. Catal. 40 (1998) 608.
[10] S. Sugiyama, Y. Hirata, T. Osaka, T. Moriga, K. Nakagawa, K.-I. Sotowa, J. Ceram. Soc. Jpn. 115 (2007) 226.
[11] S. Sugiyama, T. Hashimoto, Y. Morishita, N. Shigemoto, H. Hayashi, Appl. Catal. A 270 (2004) 253.
[12] S. Sugiyama, T. Hashimoto, Y. Tanabe, N. Shigemoto, H. Hayashi, J. Mol. Catal. A 227 (2005) 255.
[13] S. Sugiyama, T. Osaka, Y. Hirata, Y. Kondo, K. Nakagawa, K.-I. Sotowa, J. Chem. Eng. Jpn. 40 (2007) 1064.
[14] T. Hattori, Catalyst Design (Shokubai Sekkei), Kodansha, Tokyo, 1989, pp. 163–166.
[15] A. Ankudinov, B. Ravel, J.J. Rehr, S.D. Conradson, Phys. Rev. B 58 (1998) 7565.
[16] K.S. Kim, A.F. Gossmann, N. Winograd, Anal. Chem. 46 (1974) 197.
[17] G. Kumar, J.R. Blackburn, R.G. Albridge, W.E. Moddeman, M.M. Jones, Inorg. Chem. 11 (1972) 296.
[18] B.M. Choudary, K.R. Kumar, Z. Jamil, G. Thyagarajan, J. Chem. Soc. Chem. Commun. (1985) 931.
[19] C.D. Wagner, W.M. Riggs, L.E. Davis, J.F. Moulder, G.E. Muilenberg, Handbook of X-Ray Photoelectron Spectroscopy, Physical Electronics Division, Perkin-Elmer Corp., Minnesota, 1979.
[20] X. Wang, H. Zhang, W. Sinker, K.R. Poeppelmeier, L.D. Marks, J. Alloys Compd. 270 (1998) 88.
[21] A.G. Sault, J.A. Ruffner, J.E. Mudd, Catal. Lett. 76 (2001) 177.
[22] S. Sugiyama, T. Hashimoto, N. Shigemoto, H. Hayashi, Catal. Lett. 89 (2003) 229.
[23] K. Shimizu, S. Koizumi, T. Hatamachi, H. Yoshida, S. Komai, T. Kodama, Y. Kitayama, J. Catal. 228 (2004) 141.
[24] K. Okumura, K. Nota, K. Yoshida, M. Niwa, J. Catal. 213 (2005) 245.
[25] K.-I. Sotowa, N. Shiraishi, Y. Iguchi, S. Sugiyama, Chem. Eng. Sci. 63 (2008) 2690.